AIP Journal of Applied Physics

Semiconductor/dielectric half-coaxial nanowire arrays for large-area nanostructured photovoltaics

X. Hua, Y. Zeng, and W. Z. Shen

Citation: Journal of Applied Physics **115**, 124309 (2014); doi: 10.1063/1.4869915
View online: http://dx.doi.org/10.1063/1.4869915
View Table of Contents: http://scitation.aip.org/content/aip/journal/jap/115/12?ver=pdfcov
Published by the AIP Publishing

Semiconductor/dielectric half-coaxial nanowire arrays for large-area nanostructured photovoltaics

X. Hua,[1,2] Y. Zeng,[1,2] and W. Z. Shen[1,2,a)]
[1]*Department of Physics and Astronomy, Institute of Solar Energy, Shanghai Jiao Tong University, 800 Dong Chuan Road, Shanghai 200240, People's Republic of China*
[2]*Laboratory of Condensed Matter Spectroscopy and Opto-Electronic Physics, Key Laboratory of Artificial Structures and Quantum Control (Ministry of Education), Department of Physics and Astronomy, Shanghai Jiao Tong University, 800 Dong Chuan Road, Shanghai 200240, People's Republic of China*

(Received 16 January 2014; accepted 18 March 2014; published online 27 March 2014)

We present a simple assembly strategy of single nanowires (NWs) to form half-coaxial nanowire arrays (NWAs) which can be easily realized in large size by standard pattering and deposition techniques. Through the finite-difference time-domain simulation, we show that the proposed half-coaxial NWAs effectively preserve the leaky modes resonances within single NWs and consequently achieve strong absorption enhancement under optimization of various structural factors. The best half-coaxial NWAs with 100 nm thick absorbing shell offer equivalent light absorption of more than 400 nm thick planar film. Benefiting from the >75% cut of the required thickness of the absorbing layer, the performances of the demonstrated half-coaxial NWAs based *a*-Si thin film solar cell also gain significant improvement. © *2014 AIP Publishing LLC*. [http://dx.doi.org/10.1063/1.4869915]

I. INTRODUCTION

Over the past decade, extensive studies of single semiconductor nanowires (NWs) have explored their great potential as a viable candidate platform for new generation photovoltaic applications.[1–5] The subwavelength dimension of the single NWs allows unique optical properties such as broad-band and angle-independent absorption as compared to bulk materials, presenting exciting advantages like use of less abundant materials or cheaper substrates.[3,4] Nevertheless, the single NWs can only serve as the nanoscale power sources,[5] and one must consider the assembly and scaling of these functional elements into arrays as required for general purpose solar devices. Although several integration structures to form the basis of solar cells have been proposed, such as the vertically stacked "multi-junction"[1,6] and parallelly integrated multi-NWs design,[6–8] their absorption is still much lower than the theoretical limits and can be improved by further optimization. More importantly, these advanced designs involve complex synthesis which is quite expensive and difficult to utilize in large area. Consequently, it would be of great importance to implement easy and conventional fabrication while well preserving the excellent absorption of single NWs, which addresses great prospects for high-efficiency and low-cost nanostructured photovoltaic applications.

In this paper, we present the half-coaxial nanowire arrays (NWAs) as a simple and general assembly strategy for large-area nanostructured photovoltaics through standard thin film deposition and patterning technologies. We have demonstrated that the half-coaxial structure of dielectric core/absorbing shell on dielectric substrate can effectively preserve the leaky modes resonances (LMRs) of single NWs, yielding excellent absorption enhancement. We also fundamentally discuss the effects of various structural factors and dielectric coatings for further improvement. As a result, a 100 nm thick absorbing shell of the optimized NWAs design offers an equivalent absorption of more than 400 nm thick planar film, reducing >75% absorbing layer thickness. Moreover, we apply the NWAs structure to amorphous silicon (*a*-Si) thin film solar cells which dramatically declines the thickness of the absorbing intrinsic layer, obtaining 13.5% and 1.79% absolute increase of fill factor *FF* and conversion efficiency η compared to the planar structure *a*-Si thin film solar cell.

II. MODELING DETAILS

We have performed the finite-difference time-domain (FDTD) simulation[9] to calculate the light absorption in all structures throughout this paper. For the single SiO_2 (core)/*a*-Si (shell) cylinder NWs, rectangular NW, and building block of half-coaxial NWAs on SiO_2 substrate in Figure 1(a), the simulation box is set as $0.6(x) \times 0.6(y) \times 0.5(z)$ μm (see the x, y, z axes in Fig. 1(a)). The periodic boundary condition is used in z direction to treat the NWs as infinitely long, which has been well applied to describing the light scattering and absorption of various single NWs.[7,10] The light source is a broadband (300–1200 nm) plane wave perpendicular to NWs axis (along in y-axis), covering the major solar spectrum AM1.5. The mesh grid is set to 3 nm over the entire simulation volume, with a refinement of 2 nm over the volume occupied by the absorbing material. The absorbed and reflected power is calculated by means of frequency-domain transmission monitors positioned around the material volume. A two dimensional frequency-domain field monitor cross-cutting the NWs in centre is utilized to obtain the electric field intensity distribution (discussed later in Fig. 1(c)). The complex refractive indices *n*, *k* of *a*-Si shell are taken from literature[11] and

a)Author to whom correspondence should be addressed. Electronic mail: wzshen@sjtu.edu.cn

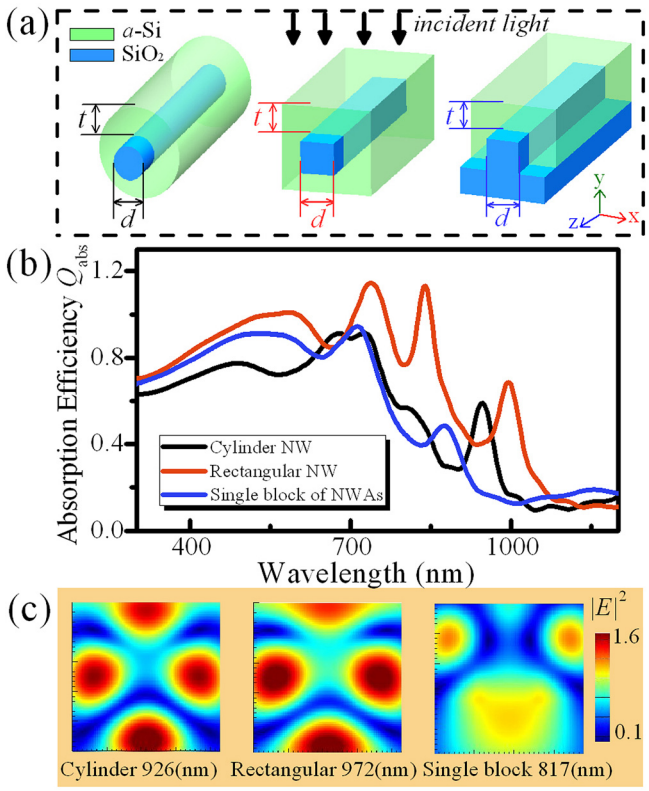

FIG. 1. (a) Schematic dielectric SiO_2 (core)/*a*-Si (shell) structures for single cylinder NW (left), rectangular NW (middle), and building block of half-coaxial NWAs on SiO_2 substrate (right). (b) Calculated spectra of the absorption efficiency Q_{abs} versus wavelength λ for the three structures ($d = 100$ nm, $t = 100$ nm). (c) Cross-sectional electric field distributions of TM_{21} mode for single cylinder NW at $\lambda = 926$ nm, rectangular NW at $\lambda = 972$ nm, and building block of NWAs at $\lambda = 817$ nm.

widely adopted in solar device modeling,[10,12] while the dielectric SiO_2 core is considered as $n = 1.5$ and has no contribution to absorption because of the large band gap.

For the NWAs structure in Figs. 2–4, the FDTD calculation utilizes a simulation box of $p(x) \times 2.1(y) \times 0.7(z)$ μm (p denotes the period of the NWAs, discussed later in Fig. 2) with periodic boundary conditions in x and z direction and perfectly matched layer condition in y direction. The reflected power R and transmitted power T normalized to the incident light power are obtained through the frequency-domain transmission monitors positioned at the top and bottom of simulation region in x-z plane, while the absorbed power A is calculated as $A = 1 - R - T$. The thickness of SiO_2 substrate is set as 0.1 μm for fast modeling. Other modeling parameters follow the same as stated above.

III. RESULTS AND DISCUSSIONS

Fig. 1(a) shows the schematics of the dielectric SiO_2 (core)/*a*-Si (shell) structures for a single typical cylinder NW, rectangular NW, and building block of half-coaxial NWAs on SiO_2 substrate, respectively. The core/shell structure can be characterized by the core diameter d and the absorbing shell thickness t. Note that though we focus on *a*-Si here for demonstration, many other absorbing semiconductor materials can be applied in the structures. In Fig. 1(b), we illustrate the calculated spectra of the absorption efficiency Q_{abs}, i.e., the absorption cross-section normalized to the geometrical cross-section,[10,13] for the three core/shell structures with $d = 100$ nm and $t = 100$ nm. Here, the unpolarized sunlight $Q_{abs} = (Q_{abs}^{TM} + Q_{abs}^{TE})/2$, where Q_{abs}^{TM} and Q_{abs}^{TE} denote absorption efficiencies for transverse-magnetic (TM, electric field parallel to the NWs axis) and transverse-electric (TE, electric field perpendicular to the NWs axis) illuminations, respectively. In the single cylinder NWs, we can clearly observe distinct resonant peaks corresponding to the LMRs occurred in subwavelength structures.[4,7] These LMRs remain in the rectangular NWs, with the observed differences of Q_{abs} primarily due to the different volumes of absorbing material in the structure. The excited resonances are of the same type which can be evidenced from the internal electric field distributions of a typical mode TM_{21} for the cylinder (at wavelength $\lambda = 926$ nm) and rectangular (at $\lambda = 972$ nm) cases,[4] as shown in Fig. 1(c). This similarity indicates the well preservation of the LMRs in rectangular morphology.

However, practical solar devices should require the assembly and scaling of these single cylinder and rectangular elements into arrays, which always involve complex synthesis. Here, we present a simple assembly strategy for high-efficiency nanostructured photovoltaic application in large size. We integrate the rectangular core/shell structures with a dielectric substrate to form the half-coaxial NWAs (see Fig. 2(a)), which can be easily realized through standard technologies of thin film deposition of *a*-Si shell on patterned SiO_2 substrate. Specifically, the nanoscale patterned substrate may be prepared in centimeter scale by various conventional nanolithography methods such as near-field, two-photon, and nanoimprint lithography with a resolution of <200 nm,[14] and the following depositing of the absorbing shell can be completed through plasma enhanced chemical vapor deposition (PECVD) and hot wire chemical vapor deposition (HWCVD). It should be noted that the deposition of semiconductor layer needs to be very carefully treated to be uniform and of high material quality, since the patterned dielectric substrate makes more difficulty on material growth compared to the planar condition. The deposition process of the half-coaxial NWAs fabrication can refer to the conventional deposition techniques utilized in *a*-Si thin film solar cells[15] and heterojunction with intrinsic thin layer (HIT) solar cells,[16] which are capable of obtaining thin *a*-Si layer (<400 nm thick) with satisfactory quality on surface textured substrate. We have also experimentally succeeded in achieving uniformly coverage of SiN_x layer (~ 80 nm thick) upon SiO_2 dielectric layer on vertically oriented NWAs through PECVD to form SiO_2/SiN_x stack passivation,[17] which supports the practicality of high quality deposition on patterned dielectric substrate. Compared to those complicated assembly strategies limited in few periods,[1,6] the NWAs are attainable on an area of several inches which is relatively large size for the nanostructured photovoltaics[17] because of the homogeneousness difficult to control.

Fig. 1(b) also presents the Q_{abs} of the single building block of the half-coaxial NWAs. Below the wavelength of 800 nm, we find similar resonant peaks to cylinder and rectangular NWs though the building block actually has smaller absorbing volume, implying the efficient preservation of the LMRs in NWAs. On the other hand, the resonances broaden

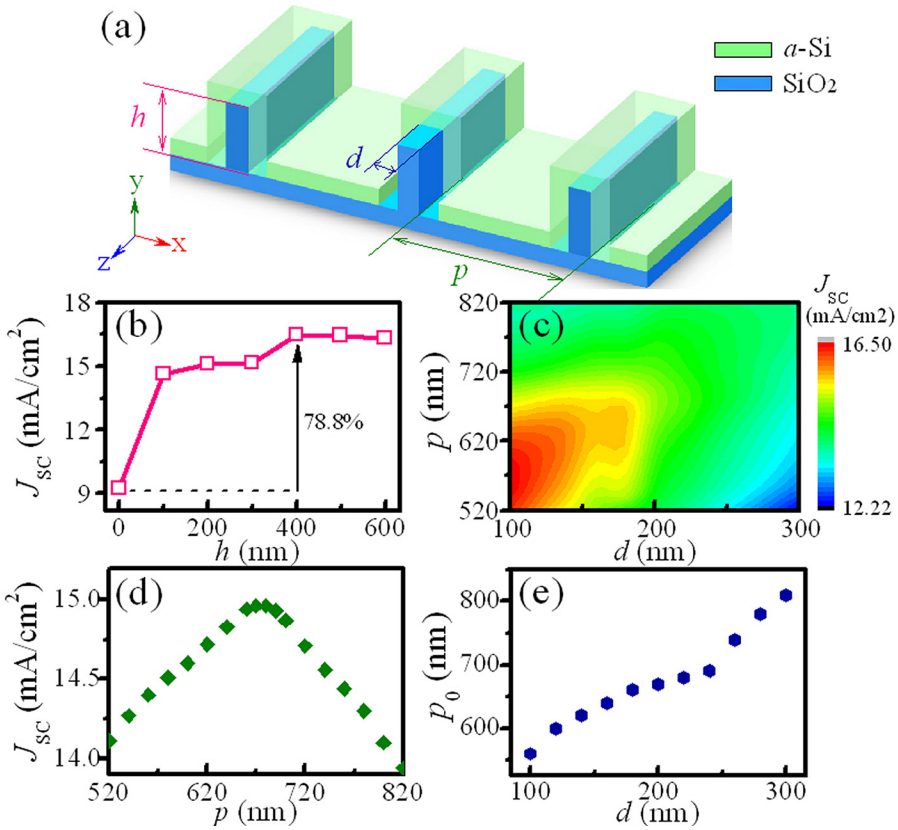

FIG. 2. (a) Schematic design of the half-coaxial SiO_2 (core)/*a*-Si (shell) NWAs. (b) The integrated short-circuit current density J_{SC} versus core height *h*. (c) The period *p* and core diameter *d* dependences of J_{SC}. (d) The *p* dependence of J_{SC} under $d = 200$ nm. (e) The best period p_0 under different *d*.

and decrease in the wavelength range >800 nm, since the low-order LMRs (TM_{21}/TE_{11}, TM_{11}/TE_{01}) are much sensitive as they extend further out of NWs and into the underlying substrate,[4] as shown in the resonance pattern (at $\lambda = 817$ nm) in Fig. 1(c). Although for the demonstrated *a*-Si shell, the absorption beyond the wavelength of 712 nm (1.74 eV, the band gap of *a*-Si), which mainly comes from defect states and interband absorption, has no contribution to

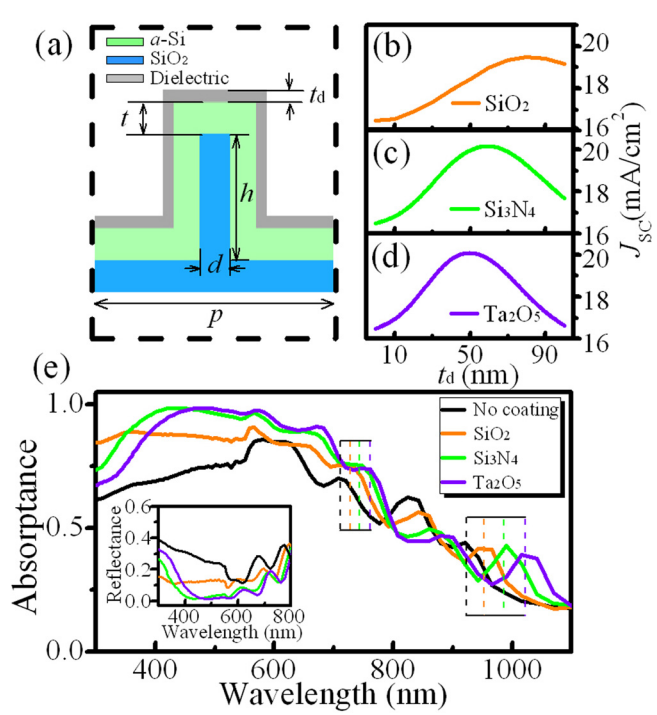

FIG. 3. (a) Cross-section drawn of the NWAs with dielectric coating. (b)–(d) The J_{SC} versus dielectric coating thickness t_d for SiO_2 (orange), Si_3N_4 (green), and Ta_2O_5 (violet). (e) Absorption spectra for SiO_2, Si_3N_4, Ta_2O_5 coated NWAs with the same $t_d = 50$ nm. Inset: Reflection spectra for SiO_2, Si_3N_4, and Ta_2O_5 coated NWAs with the same $t_d = 50$ nm.

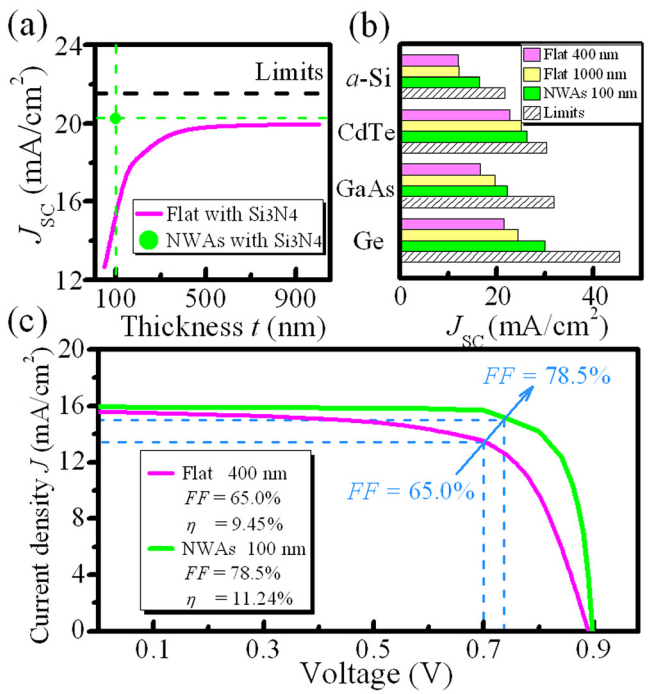

FIG. 4. (a) J_{SC} versus *a*-Si thickness *t* for flat films with Si_3N_4 coating, the J_{SC} of $t = 100$ nm NWAs and the theoretical limits are also indicated. (b) The J_{SC} of $t = 400$ nm, $t = 1000$ nm flat film, $t = 100$ nm NWAs, and the theoretical limits, for four absorbing materials *a*-Si, CdTe, GaAs, and Ge. (c) The *J*-*V* curves of $t = 400$ nm flat structure and $t = 100$ nm NWAs structure *a*-Si thin film solar cells under AM1.5 spectrum.

photogenerated current, we can still see considerable light trapping enhancement by LMRs in the long wavelength region, showing greater potentials for semiconductors with small band gap (discussed later in Fig. 4(b)).

Then, we assemble the single building blocks to form the half-coaxial NWAs. The schematic design is shown in Fig. 2(a) together with the influencing factors of light absorption in the structure, i.e., the core height h, period of arrays p, and core diameter d, where the thickness of a-Si absorbing shell is fixed at $t = 100$ nm. Fig. 2(b) gives out the h dependence of the integrated short-circuit current density J_{SC} of the NWAs with $d = 100$ nm and $p = 550$ nm. Note that the J_{SC} is the total photogenerated current without any electrical loss, which is integrated under AM1.5 spectrum (absorption below the band gap of absorbing material is not included) as $J_{SC} = q\int \Gamma(\lambda)Abs(\lambda)d\lambda$, where q is the elementary charge, Γ is the photon flux density, and $Abs(\lambda)$ denotes the absorptance of the structure as a function of wavelength λ. We can see that the J_{SC} increases with h and reaches the maximal $J_{SC} = 16.47\,mA/cm^2$ at $h = 400$ nm, obtaining a 78.8% enhancement compared to the flat condition of $h = 0$. With the optimized h fixed at 400 nm, we calculate the p and d dependences of J_{SC}, as shown in Fig. 2(c). Clearly, the J_{SC} always climbs with increasing p until the peak value and then declines sharply (see the demonstrated p-dependence of J_{SC} under $d = 200$ nm in Fig. 2(d)), which corresponds closely to the results in literature.[7] This behaviour comes from the total light interaction effect of the periodic arrays, which is to some extent similar to the light coupling and propagations within the one-dimensional gratings based structure.[18,19] The Febry-Pérot phase-matching resonances originated from the coupling of Bloch modes[18,19] and Rayleigh anomaly[20] comprehensively determine the light absorption. Besides, the d also plays the crucial role on absorption properties because it dominates the LMRs in every single block of NWAs.[12] Normally, smaller d exhibits stronger absorption since the absorbing shell occupies higher volume proportion and the light primarily concentrates in the centre part. However, large d also owns advantage due to the more LMRs allowed in the structure. As a result, $d = 100$ nm (with the highest $J_{SC} = 16.49\,mA/cm^2$ at $p = 560$ nm) is a balanced diameter to optimize the NWAs absorption which is feasible for patterning technology. In addition, we show the relationship of d and the best period p_0 under different d in Fig. 2(e), which is approximately linear and can be used for rough evaluation.

Moreover, we introduce the dielectric coating upon a-Si shell (see the cross-section drawn in Fig. 3(a)) to provide excellent light trapping in the half-coaxial NWAs, which has already been proved very effective for single NWs.[12] Figs. 3(b)–3(d) present the J_{SC} as a function of the thickness of the dielectric coatings t_d for SiO_2 ($n = 1.5$), Si_3N_4 ($n = 2.0$), and Ta_2O_5 ($n = 2.3$), respectively, on the well-established configuration presented above ($t = 100$, $h = 400$, $p = 560$, and $d = 100$ nm). It is found that the dielectric coatings can substantially enhance the J_{SC} by $\sim 20\%$ than the NWAs without coating ($t_d = 0$). Among the three coating materials, the J_{SC} attains maximum at different t_d (for SiO_2 80 nm, Si_3N_4 60 nm, and Ta_2O_5 50 nm), while the Si_3N_4 seems to be the best choice, achieving the extremely high $J_{SC} = 20.24\,mA/cm^2$. In Fig. 3(e), we illustrate the detailed absorption spectra of the dielectric coatings with the same $t_d = 50$ nm for SiO_2, Si_3N_4, and Ta_2O_5, respectively. The long wavelength absorptance below a-Si band gap is also shown to better explain the light trapping mechanism of dielectric coatings. Compared to the no dielectric coating condition, the absorptance considerably enhances below the wavelength of 800 nm, while little augment can be found above the wavelength of 800 nm. Besides, the n-driven red-shifts of resonance peaks become larger with increasing wavelength as marked by dash boxes in Fig. 3(e). This absorption behavior matches well with the results of single NWs[12] and therefore we believe that the enhancement arises from not only antireflection coating, but also the Fano interference effect[21] in single NWs.[12,22] For $\lambda > 800$ nm, the dielectric coating does not play much role in the light absorption enhancement compared to the strong LMRs which have not been severely coupled into the substrate. Whereas, for weak LMRs in $\lambda < 800$ nm, the incident light is localized via constructive interference with the reflected light, resulting in strong absorption enhancement. The enlarged n-driven red-shifts with increasing wavelength are attributed to the increased phase shifts of the interference between the incident light and the reflected light. The reflection spectra of the three coatings are also presented as a reference in the inset of Fig. 3(e), demonstrating the simultaneous excellent antireflection performance of the half-coaxial NWAs like other nanostructures.[23,24]

By synthetically combining all the effects of the light interaction in periodic arrays, the LMRs of single blocks, and the Fano interference effect introduced by dielectric coatings, we can obtain the optimal $J_{SC} = 20.24\,mA/cm^2$ for the half-coaxial NWAs with only $t = 100$ nm a-Si absorbing shell. For comparison, we demonstrate in Fig. 4(a) the t-dependent J_{SC} of a-Si flat film with the same Si_3N_4 coating $t_d = 60$ nm. Critically, it requires more than 400 nm thick a-Si (the typical thickness for a-Si thin film solar cells) to produce a comparable J_{SC} for the planar structure, indicating a $> 75\%$ decline of the thickness of absorbing layer. In consideration of the increased surface area of NWAs structure, the volume of the absorbing material used can also be cut by 39%. Furthermore, the half-coaxial NWAs structure can generally apply to diverse kinds of materials to reduce the thickness of absorbing layers. Fig. 4(b) shows the J_{SC} of $t = 400$ nm, $t = 1000$ nm flat films, $t = 100$ nm NWAs and the theoretical limits, for different materials (a-Si, CdTe, GaAs, and Ge)[11] widely used in optoelectronic devices. Note that all the structure parameters are fixed as the optimized configuration above ($t = 100$, $h = 400$, $p = 560$, and $d = 100$ nm) except the dielectric coating to avoid its influence. We can see that the proposed half-coaxial NWAs with 100 nm absorbing shell yields higher J_{SC} than those 1000 nm thick planar films for all four materials, revealing its great prospects in saving absorbing materials, especially for the rare elements which cost rather high.

Finally, we extend the half-coaxial NWAs structure into solar cells to see the advantages brought by thinner absorbing layer. We again take a-Si thin film solar cells for demonstration. In Fig. 4(c), we calculate the J-V curves of $t = 400$ nm (p(10 nm)/i(380 nm)/n(10 nm)) flat structure and

$t = 100$ nm (p(10 nm)/i(80 nm)/n(10 nm)) half-coaxial NWAs structure solar cells with both 60 nm Si_3N_4 coatings through AFORS-HET (numerical simulator automat for simulations of heterojunctions).[25] We have set the illumination as AM1.5 spectrum and the optical band gap of *a*-Si to be 1.74 eV. The n type and p type doping concentrations are both 7×10^{19} cm^{-3}, and the electron mobility μ_n and hole mobility μ_p are fixed as 5 and 1 cm^2/V s, respectively. Other required electrical parameters and the detailed *a*-Si defects like bandtail and dangling-bonds defects are all picked from the elaborate model in literature[25] to ensure the reliability, while the contacts are assumed as Ag contact and flatband. For the $t = 400$ nm flat structure *a*-Si thin film solar cell, we obtain the open-circuit voltage $V_{OC} = 0.89$ V, $J_{SC} = 15.6$ mA/cm^2, $FF = 65.0\%$, $\eta = 9.45\%$. These results are quite comparable to the performances of experimental *a*-Si thin film solar cell ($V_{OC} = 0.89$ V, $J_{SC} = 16.8$ mA/cm^2, $FF = 67.0\%$, and $\eta = 10.1\%$),[15] while the J_{SC} exhibits smaller since we have not considered additional light trapping texture except the Si_3N_4 coating, which results in the slightly lower *FF* and η. Thus, we believe that this electrical solar cell model is proper and convincing to study the effects of reducing *a*-Si layer thickness in thin film solar cell. Then for $t = 100$ nm half-coaxial NWAs structure thin film solar cell, we can find that the yielded $FF = 78.5\%$ and $\eta = 11.24\%$ are improved by 21% and 19%, respectively, compared to the above flat structure, while the $V_{OC} = 0.90$ V and $J_{SC} = 16.0$ mA/cm^2 show slender increment. The improvement of solar cell performance can be interpreted by the dramatic decline (300 nm) of the required thickness of the absorbing intrinsic *a*-Si layer which severely limits *FF* and therefore η due to its high resistivity and bulk recombination. The ~75% cut of the *a*-Si intrinsic layer thickness leads to much shorter collection distance for charge carriers and lower resistance, which produce higher *FF* and comprehensively enhance the solar cell performances. Importantly, it should be noted that although other resistance issues like contact and shunting in realistic situation may affect the *FF*, the proposed half-coaxial NWAs based solar cell provides a novel approach to overcome the low *FF* problem in nanostructured solar cells by reducing the necessary thickness of the absorbing layer, showing great potential in realizing breakthrough for high-efficiency nanostructured solar cells.

IV. CONCLUSIONS

We have proposed the half-coaxial NWAs as an easy integration design of single NWs which is potentially scalable to large-area modules by standard patterning technology and thin film deposition. From the FDTD simulation of the structure of dielectric core/absorbing shell on dielectric substrate, we have demonstrated that the light absorption can be significantly enhanced by carefully optimizing the core height, period, core diameter, and the influences of dielectric coatings. This strong enhancement indicates that the half-coaxial NWAs scheme effectively retains the high absorption of single elements, and allows us to obtain the J_{SC} of up to 20.24 mA/cm^2 with only 100 nm thick *a*-Si absorbing shell which would otherwise require more than 400 nm thick *a*-Si for planar thin films, leading to a >75% cut of the absorbing layer thickness. This structure can also generally apply to a wide range of absorbing materials to save ~40% semiconductor volume. Moreover, this proposal serves as an effective solution for the low *FF* problem of the nanostructured solar cells to make a breakthrough in high efficiency because of the greatly reduced thickness of the absorbing layer. As a result, we can achieve $FF = 78.5\%$ and $\eta = 11.24\%$ in the half-coaxial NWAs based solar cell, which obtain 13.5% and 1.79% absolute increase compared to the planar structure *a*-Si thin film solar cell.

ACKNOWLEDGMENTS

This work was supported by National Major Basic Research Project (No. 2012CB934302), and Natural Science Foundation of China (Nos. 11174202 and 61234005).

[1]T. J. Kempa, R. W. Day, S.-K. Kim, H.-G. Park, and C. M. Lieber, Energy Environ. Sci. **6**, 719 (2013).
[2]B. Tian, T. J. Kempa, and C. M. Lieber, Chem. Soc. Rev. **38**, 16 (2009).
[3]M. M. Adachi, M. P. Anantram, and K. S. Karim, Nano Lett. **10**, 4093 (2010).
[4]L. Cao, J. S. White, J.-S. Park, J. A. Schuller, B. M. Clemens, and M. L. Brongersma, Nature Mater. **8**, 643 (2009).
[5]B. Tian, X. L. Zheng, T. J. Kempa, Y. Fang, N. F. Yu, G. H. Yu, J. L. Huang, and C. M. Lieber, Nature **449**, 885 (2007).
[6]T. J. Kempa, J. F. Cahoon, S.-K. Kim, R. W. Day, D. C. Bell, H.-G. Park, and C. M. Lieber, Proc. Natl. Acad. Sci. U.S.A. **109**, 1407 (2012).
[7]L. Cao, P. Fan, A. P. Vasudev, J. S. White, Z. Yu, W. Cai, J. A. Schuller, S. Fan, and M. L. Brongersma, Nano Lett. **10**, 439 (2010).
[8]D. Tham and J. R. Heath, Nano Lett. **10**, 4429 (2010).
[9]FDTD Solutions 8.0, Lumerical 2012.
[10]W. F. Liu, J. I. Oh, and W. Z. Shen, Nanotechnology **22**, 125705 (2011).
[11]E. D. Palik, *Handbook of Optical Constants of Solids* (Academic, New York, 1985).
[12]W. F. Liu, J. I. Oh, and W. Z. Shen, IEEE Electron Device Lett. **32**, 45 (2011).
[13]C. F. Bohren and D. R. Huffman, *Absorption and Scattering of Light by Small Particles* (Willey, New York, 1998).
[14]P. N. Prasad, *Nanophotonics* (John Wiley & Sons, Inc., 2004).
[15]S. Benagli, D. Borrello, E. Vallat-Sauvain, J. Meier, U. Kroll, J. Hötzel, J. Spitznagel, J. Steinhauser, L. Castens, and Y. Djeridane, in *24th European Photovoltaic Solar Energy Conference, Hamburg, September 2009*, pp. 2293–2298.
[16]M. Taguchi, A. Yano, S. Tohoda, K. Matsuyama, Y. Nakamura, K. Nishiwaki, K. Fyjita, and E. Maruyama, IEEE J. Photovoltaics **4**, 96 (2014).
[17]X. X. Lin, X. Hua, Z. G. Huang, and W. Z. Shen, Nanotechnology **24**, 235402 (2013).
[18]P. Lalanne, J. P. Hugonin, and P. Chavel, J. Lightwave Technol. **24**, 2442 (2006).
[19]S. Bandiera, D. Jacob, T. Muller, F. Marquier, M. Laroche, and J.-J. Greffet, Appl. Phys. Lett. **93**, 193103 (2008).
[20]L. Rayleigh, Philos. Mag. **14**, 60 (1907).
[21]U. Fano, Phys. Rev. **124**, 1866 (1961).
[22]E. Miroshnichenko, Phys. Rev. A **81**, 053818 (2010).
[23]P. Spinelli, M. A. Verschuuren, and A. Polman, Nat. Commun. **3**, 692 (2012).
[24]W. Q. Xie, W. F. Liu, J. I. Oh, and W. Z. Shen, Appl. Phys. Lett. **99**, 033107 (2011).
[25]X. Hua, Z. P. Li, W. Z. Shen, G. Y. Xiong, X. S. Wang, and L. J. Zhang, IEEE Trans. Electron Devices **59**, 1227 (2012).